BIOCHEMISTRY
including biophysical chemistry & molecular biology
Article

Biochemistry **2009,** *48,* 5389–5395 5389
DOI: 10.1021/bi900346m

Mechanistic Variations among Reverse Transcriptases of Simian Immunodeficiency Virus Variants Isolated from African Green Monkeys[†]

Mark Skasko,[‡] Tracy L. Diamond,[§] and Baek Kim*

Department of Microbiology and Immunology, University of Rochester Medical Center, 601 Elmwood Avenue, Box 672, Rochester, New York 14642[‡] Current address: Department of Pathology, University of California at San Diego, 9500 Gilman Dr., Dept 0679, La Jolla, CA 92093-0679. [§] Current address: Merck & Co., Inc., WP26A-3000, 770 Sumneytown Pike, P.O. Box 4, West Point, PA 19486-0004

Received February 27, 2009; Revised Manuscript Received April 27, 2009

ABSTRACT: Here we report enzymatic variations among the reverse transcriptases (RTs) of five simian immunodeficiency virus (SIV) strains, Sab-1, 155-4, Gri-1, 9063-2, and Tan-1, which were isolated from four different species of naturally infected African green monkeys living in different regions across Africa. First, Sab-1 RT exhibits the most efficient dNTP incorporation efficiency at low dNTP concentrations, whereas the other four SIVagm RT proteins display different levels of reduced polymerase activity at low dNTP concentrations. Tan-1 RT exhibited the most restricted dNTP incorporation efficiency. Indeed, the pre-steady state analysis revealed that Sab-1 RT displays tight dNTP binding affinity ($K_d \sim 1-5\,\mu M$), comparable to values observed for NL4-3 and HXB2 HIV-1 RTs, whereas the dNTP binding affinity of Tan-1 RT is 6.2, ~34.8-fold lower than that of Sab-1 RT. Second, Tan-1 RT fidelity was significantly higher than that of Sab-1 RT. Indeed, Tan-1 RT enzymatically mimics oncoretroviral murine leukemia virus RT which is characterized by its low dNTP binding affinity and high fidelity. This study reports that simultaneous changes in dNTP binding affinity and fidelity of RTs appear to occur among natural SIV variants isolated from African green monkeys.

Genomic hypervariability is known to be a powerful evolutionary tool of lentiviruses, and the amino acid sequence variations are observed throughout viral coding sequences (*1*−*3*). However, the resulting functional and mechanistic changes of the viral gene products, which can be induced by viral hypermutagenesis, have been limitedly documented among natural viral isolates. The envelope protein of lentiviruses such as human and simian immunodeficiency viruses (HIV-1 and SIV, respectively) has been a major research subject for delineation of viral genomic mutations and consequential molecular and functional alterations (*4*, *5*), which explain viral cell tropism changes between macrophages and CD4+ T cells during the course of viral pathogenesis (*6*, *7*). The mechanistic and structural changes of HIV-1 reverse transcriptase (RT) and protease (PR) among drug resistant viral populations have been studied mainly for the mechanisms which render them resistant to antiviral drugs. However, neither biochemical variations of RT and PR variants encoded in natural lentivirus isolates nor their virological impacts have been addressed.

In this study, we searched for functional alterations among RTs encoded in naturally infective SIV strains. For this, we chose five SIV strains previously isolated as representative clones from four different species of naturally infected African green monkey (AGM) superspecies, *Chlorocebus sabaeus* (Sab-1), *Chlorocebus pygerythrus* (155-4 and 9063-2), *Chlorocebus aethiops* (Gri-1), and *Chlorocebus tantalus* (Tan-1). These four AGM species live in uniquely different regions of Africa, and the infection of these SIVagm strains does not cause disease in their AGM hosts. Previous works estimate the genetic diversity of some SIVagm population to exceed that of all other primate lentiviruses (*8*−*13*). Moreover, a recent genetic analysis of both viruses and hosts suggested that SIVagm infection of AGM may have occurred after the AGM superspecies diverged into the four subspecies through horizontal interspecies infections (*14*). This contradicts the previous thought that SIV infected an ancestor of green monkeys before the AGM lineage split (*15*).

In this study, we unexpectedly observed significant enzymatic variations among RTs of the five SIVagm strains. Specifically, RTs of Sab-1 and Tan-1 displayed the largest differences in their dNTP utilization efficiency, dNTP binding affinity, and enzyme fidelity. This observation reveals that, as observed in the Env variants both within and between hosts, RT can also undergo mechanistic changes that may contribute to viral life cycle.

MATERIALS AND METHODS

Plasmids, Cells, and Chemicals. *Escherichia coli* DH5α (Invitrogen) was used for the construction and amplification

[†]This work was supported by National Institutes of Health (NIH) Grant AI049781 (B.K.) and NIH Grant T32 AI49815 (M.S.).

*To whom correspondence should be addressed: Department of Microbiology and Immunology, University of Rochester Medical Center, 601 Elmwood Ave., Box 672, Rochester, NY 14642. Telephone: (585) 275-6916. Fax: (585) 473-9573. E-mail: baek_kim@urmc.rochester.edu.

Published on Web 05/01/2009

of plasmids, and BL21(DE3) (Invitrogen) was used for the overexpression of SIVagm RT proteins. Protein purification reagents were purchased from Novagen. PCR reagents were purchased from Clontech, and restriction enzymes, T7 RNA polymerase, and T4 polynucleotide kinase were purchased from New England Biolabs. dNTP stock solutions were purchased from GE Heathcare.

Construction of RT Expression Plasmids and Purification of RT Protein. The SIVagm RT proteins were overexpressed in *E. coli* BL21(DE3) as described previously (*16*, *17*). The full-length SIVagm RT genes were amplified from the molecular clones of the five previously isolated SIVagm strains, Sab-1, 155-4, Gri-1, 9063-2, and Tan-1, which were kindly provided from V. Hirsh (National Institutes of Health, Bethesda, MD), and the RT genes were inserted into either pET28a or pHis-NcoI (from A. Hizi) using either NdeI or NcoI for their N-terminal ends and XhoI or HindIII for the C-terminal ends. These constructs express the full-length RT proteins with a hexahistidine tag at their N-termini. The hexahistidine-tagged RT was purified using Ni^{2+} chelation chromatography as described previously (*16*−*18*). From 1 L of culture, we were able to purify 0.5−2 mg of RT proteins. To examine the purity of the RT proteins, 1−4 μg of the purified RTs was analyzed via 10% SDS−polyacrylamide gels using 1−4 μg of 98% pure bovine serum albumin (Sigma) as a control. The gels, visualized by Coomassie staining, were analyzed by a densitometer, and the purified RT proteins exhibited similar levels of minor contaminants as the bovine serum albumin control, suggesting that the RT proteins used in this study must be at least 95% pure.

Assay for dNTP Concentration-Dependent DNA Polymerase Activity of SIVagm RT Proteins. The primer extension assay was previously described (*19*). Briefly, an RNA template/primer (T/P) was prepared by annealing a 38-mer RNA (5′-GCUUGGCUGCAGAAUAUUGCUAGCGGGAAUUCGGCGCG-3′, Dharmacon Research) to the 17-mer A primer (5′-CGCGCCGAATTCCCGCT-3′, template:primer ratio of 2.5:1) labeled with ^{32}P at the 5′-end by T4 polynucleotide kinase. Assay mixtures (20 μL) contained 10 nM T/P, RT, and dNTPs as specified in each figure legend. Reaction mixtures were incubated at 37 °C for 5 min and reactions terminated for analysis. Single or multiple amounts of RTs (i.e., 1× and 4×) were used. These reaction conditions allow multiple rounds of primer extension. Products were resolved using 14% polyacrylamide−urea gels and visualized using a PhosphorImager (GE Healthcare).

Pre-Steady State Kinetic Assays. Pre-steady state burst and single-turnover experiments were performed to examine the transient kinetics associated with incorporating a single nucleotide onto four different T/Ps (*20*). To study the incorporation of each of the four dNTPs, four different ^{32}P-labeled 23-mer primers (matched, Extend A primer, 5′-CGCGCCGAATTCCCGCTAGCAAT-3′; Extend T primer, 5′-CCGAATTCCCGCTAGCAATATT-3′; Extend G primer, 5′-CGAATTCCCGCTAGCAATATTCT-3′; Extend C primer, 5′-GCCGAATTCCCGCTAGCAATATT-3′) were individually annealed to a 38-mer RNA template (see above). Reactions were performed using a Kintek rapid quench machine (*21*−*23*). Products were analyzed on a 14% denaturing sequencing gel by electrophoresis and quantified with the Cyclone Phosphorimager (PerkinElmer Life Sciences). Pre-steady state burst experiments were employed to determine the active site concentrations of the Sab-1 and Tan-1 RT proteins on the 23-mer T primer annealed to the 38-mer RNA template. In this experiment, 800 μM dTTP was rapidly mixed with RT (50−75 nM active RTs) prebound to T/P (300 nM). In the pre-steady state single-turnover experiments that measured the dNTP concentration dependence of the purified SIVagm RTs, 200 nM active RT was added to 50 nM T/P.

Data Analysis. Pre-steady state kinetic data were analyzed using nonlinear regression. Equations were generated with KaleidaGraph version 3.51 (Synergy Software). Data points obtained during the burst experiment were fitted to the burst equation (*21*, *24*).

$$[\text{product}] = A[1 - \exp(-k_{\text{obs}}t) + k_{\text{ss}}t] \quad (1)$$

A is the amplitude of the burst, which reflects the actual concentration of enzyme that is in the active form. k_{obs} is the observed first-order rate constant for dNTP incorporation, whereas k_{ss} is the observed steady state rate constant (*21*, *22*, *25*). Data from single-turnover experiments were fit to a single-exponential equation that measures the rate of dNTP incorporation (k_{obsd}) per given dNTP concentration. These results were then used to determine K_{d}, the dissociation constant for binding of dNTP to the RT−T/P binary complex, and k_{pol}, the maximum rate of chemical catalysis and/or conformational change. This was done by fitting the data to the following equation.

$$k_{\text{obsd}} = k_{\text{pol}}[\text{dNTP}]/(K_{\text{d}} + [\text{dNTP}]) \quad (2)$$

From this equation, we could then identify the kinetic constants for each RT during pre-steady state kinetics: k_{pol}, the maximum rate of dNTP incorporation, and K_{d}, the equilibrium dissociation constant for the interaction of dNTP with the E·DNA complex (*21*, *26*).

Misincorporation Assay with Biased dNTP Pools. A matched RNA T/P was prepared by annealing the 38-mer RNA template (see above) to the 17-mer A primer (see above). Assay mixtures (20 μL) contained 10 nM T/P, the RT protein concentrations showing the primer extension activities described in the individual figure legends with only three of the four dNTPs at 250 μM. Reactions were performed as described above to examine multiple rounds of primer extension in biased dNTP environments.

Mismatched Primer Extension Assay. First, a mismatched RNA T/P was prepared by annealing the 38-mer RNA template to the mismatched 16-mer G/T primer (5′-CGCGCCGAATTCCCGT-3′), and a mismatched DNA T/P was prepared by annealing the 38-mer DNA template with the mismatched 19-mer C/A primer (5′-CGCGCCGAATTCCCGCTAA-3′). All primers used in this assay were labeled with ^{32}P at their 5′-ends (template:primer ratio of 2.5:1). Assay mixtures (20 μL) contained 10 nM T/P, the RT protein concentrations showing the primer extension activities described in the individual figure legends with all four dNTPs at 250 μM. Reactions were performed as described above to examine multiple rounds of primer extension on mismatched T/P. Concentrations of RTs (i.e., from 1× to 4×) and the dNTP concentration used in each primer extension experiment are given in each figure legend. Products were resolved on a 14% polyacrylamide−urea gel and visualized using a PhosphorImager.

RESULTS

dNTP Concentration-Dependent DNA Polymerase Activity of SIVagm RTs. We first cloned the RT gene of the five

SIVagm clones, Sab-1, 155-4, Gri-1, 9063-2, and Tan-1 (kindly provided by V. Hirsh), previously isolated from four different African green monkey species into bacterial expression plasmids. These SIVagm clones were isolated and characterized as representative clones after sequencing analysis, and these clones have been used in various virological studies (*9*, *11*, *27*−*29*). N-Terminal hexahistidine tags were added to these RT genes, and the protein was overexpressed in *E. coli* and purified using Ni^{2+}-charged agarose columns as previously described (*16*, *17*). We next examined the dNTP utilization efficiency of the five purified SIVagm RT proteins using a primer extension reaction. RNA template/DNA primer (T/P) was prepared by annealing a 38-mer RNA template to the 5′-end of a ^{32}P-labeled 17-mer primer (Figure 1), and this primer was extended by the purified Tan-1 and Sab-1 RT proteins displaying approximately 40−60% linear primer extension with a high dNTP concentration (50 μM) at 37 °C for 5 min (the first lane of each panel in Figure 1). The same reaction was then repeated using nine decreasing concentrations of dNTPs (from 50 to 0.025 μM). These reaction conditions allow multiple rounds of linear steady state primer extension during the 5 min incubation.

As shown in Figure 1, Sab-1 RT protein exhibited efficient DNA polymerization activity even at low dNTP concentrations such as 25 nM. 155-4 and Gri-1 RT proteins displayed slightly diminished activity at the low dNTP concentrations as compared to Sab-1 RT protein. Strikingly, RTs of 9063-2 and Tan-1 exhibited significant reduction in their DNA polymerase activity at lower dNTP concentrations. To quantitatively compare these variations, we determined the dNTP concentrations reducing 50% of the enzyme activity shown in 50 μM dNTP, by plotting the levels of the fully extended 38 bp product at each dNTP concentration and comparing them to that at 50 μM dNTP. The dNTP concentrations producing 50% of the activity for the five RT proteins were marked in Figure 1 with asterisks. Indeed, among the five SIVagm RT proteins, Sab-1 and Tan-1 RT exhibited the largest difference (~15-fold) in dNTP concentrations, showing 50% activity reduction, which were 75 and 1100 nM, respectively. This result supports the idea that RTs of SIVagm natural variants can enzymatically vary. In addition, these data indicate that unlike Sab-1 RT, the dNTP utilization step becomes rate-limiting for Tan-1 RT at low dNTP concentrations, which may result from the restricted dNTP binding affinity of Tan-1 RT as compared to that of Sab-1 RT.

Pre-Steady State Kinetic Analysis of SIVagm Sab-1 and Tan-1 RT Proteins. We next tested the possibility that Tan-1 RT may have reduced dNTP binding affinity as compared to Sab-1 RT. For this test, we employed pre-steady state kinetic analysis with a rapid quench instrument which allowed us to determine the dNTP binding affinity (K_d) and rate of incorporation (k_{pol}) of RT during a single round of primer extension (*21*, *22*). First, we determined the active concentrations of Sab-1 RT and Tan-1 RT on a ^{32}P-labeled 23-mer T primer annealed to the 38-mer RNA template utilizing burst assays. Determination of the active site concentration of the RT proteins allows us to ensure that there is a single round of primer extension during the pre-steady state dNTP titration reactions. In the active site concentration determination (Figure 2A), RT was prebound to 300 nM T/P and product formation was assessed after incubation with 800 μM dTTP for 5 ms to 4 s. Typically, a large burst of extended T/P (pre-steady state first-round extension) is formed followed by a more gradual formation of extended T/P (steady state multiple-round extension) (see Figure 2A). The results were

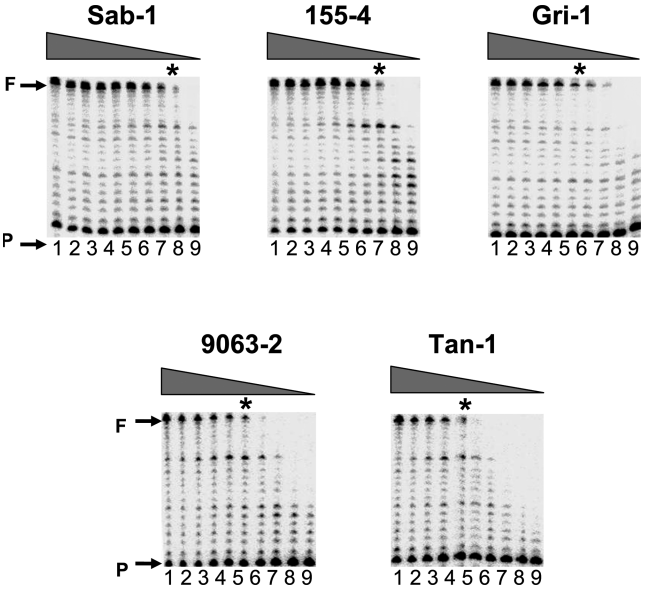

FIGURE 1: dNTP concentration-dependent DNA polymerase activity of five SIVagm RT proteins. A ^{32}P-labeled 17-mer primer (P, 5′-CGCGCCGAATTCCCGCT-3′) annealed to a 38-mer RNA template (5′-GCUUGGCUGCAGAAUAUUGCUAGCGG-GAAUUCGGCGCG-3′) was incubated with equal activities of the indicated SIVagm RT protein at 37 °C for 5 min with 50 μM dNTPs (the highest dNTP concentration, lane 1), generating approximately 40−60% full extension (F) of the primer. The same reaction was repeated with nine decreasing dNTP concentrations (25, 10, 5, 1, 0.5, 0.25, 0.1, 0.05, and 0.025 μM). The reaction mixtures were analyzed with 14% denaturing polyacrylamide gels. The dNTP concentrations exhibiting 50% of the reduction of the fully extended products, compared to the highest dNTP concentration (50 μM), were determined and marked with asterisks for each RT protein. The presented data are a representative set of our multiple qualitative experiments, and the concentrations displaying 50% of full extension remained consistent during these qualitative experiments.

fitted to the burst equation (*21*, *24*) (eq 1), and the amount of active RT was determined. Sab-1 RT and Tan-1 RT were 61.4 and 30.0% active (92.1 and 27.75 nM), respectively. The active site concentrations of RT proteins can vary depending on the purification conditions employed. However, since the single-turnover dNTP titration is determined in an excess of active RT protein with respect to the T/P, the varying active site concentrations of the purified RT proteins do not affect the pre-steady state kinetic investigation described below.

We then performed single-turnover experiments with 200 nM active RT in molar excess of T/P (50 nM). We used four different T/P complexes to assay the incorporation rate of each of the four dNTPs for Sab-1 RT and Tan-1 RT. We measured the rate of product formation (k_{obs}) at six different dNTP concentrations. The rate of product formation (k_{obs}) is plotted versus dNTP concentration to yield best-fit curves in eq 2 (*21*, *22*, *25*) (Materials and Methods and Figure 2B). These data were then used to determine the binding affinity for the incoming dNTP (K_d) and the rate of conformational change and chemical catalysis (k_{pol}). The values for all four dNTPs are summarized in Figure 2C. The binding affinity (K_d) of Sab-1 RT for incoming dNTPs is 0.3−1.2 μM, and the rate at which it incorporates a nucleotide (k_{pol}) is 0.03−0.07 s^{-1}. The rate at which Tan-1 RT incorporates a nucleotide varied by only 1.04−1.56-fold when compared to that of Sab-1 RT, while Tan-1 RT binds the incoming dNTP (K_d) with an affinity 6.2−34.8-fold lower than that of Sab-1 RT. Consequently, Tan-1 RT is 4.6−33.5-fold less

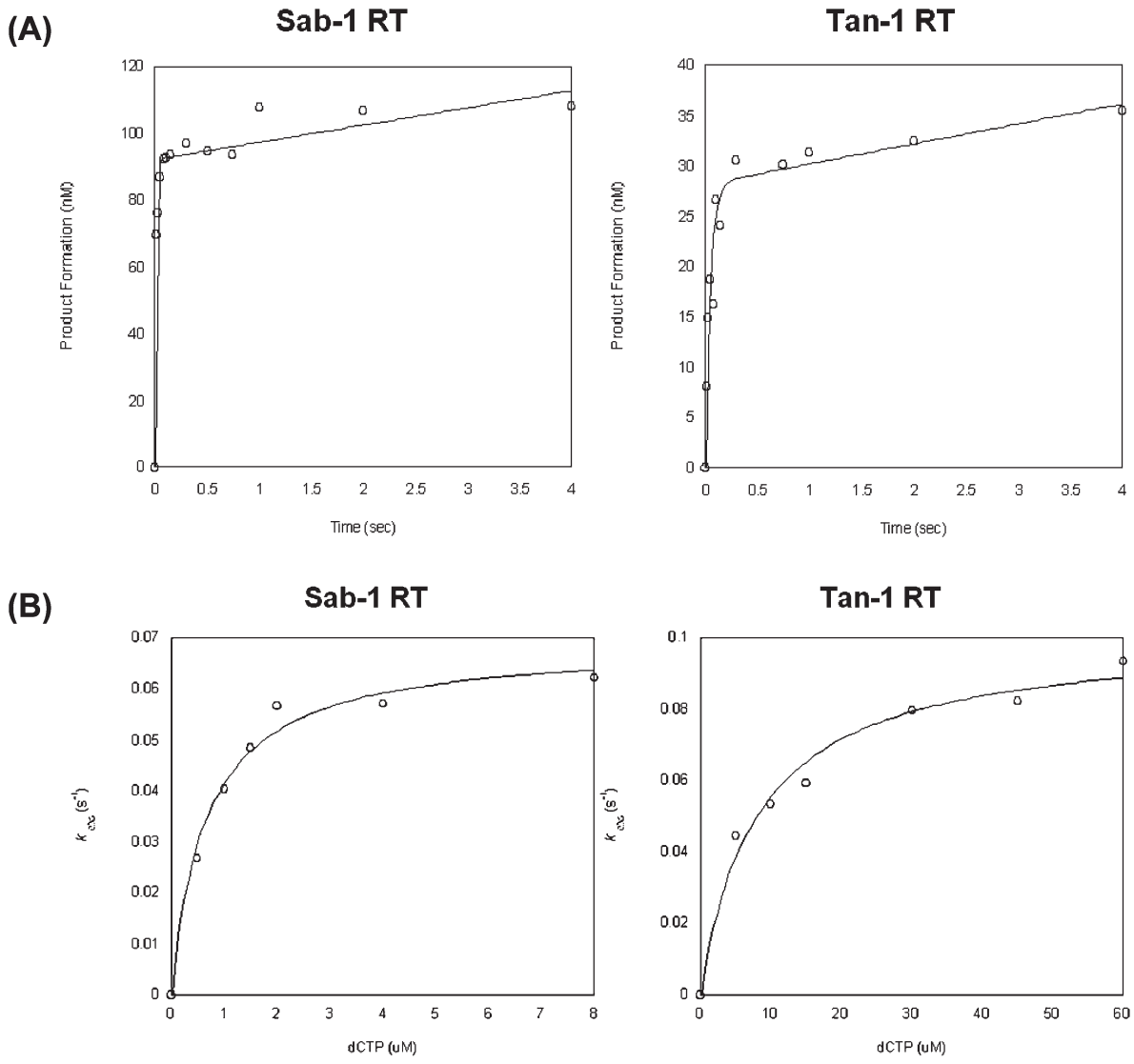

(C)

dNTP	RT	kpol (s^{-1})	fold	Kd (μm)	fold	kpol/Kd	fold
dTTP	Sab-1	0.0512 ± 0.0006	1.04	0.284 ± 0.048	34.77	0.180	33.47
	Tan-1	0.0532 ± 0.0089		9.881 ± 2.935		0.005	
dCTP	Sab-1	0.069 ± 0.0052	1.46	0.672 ± 0.096	12.23	0.103	8.37
	Tan-1	0.100 ± 0.0174		8.227 ± 3.046		0.012	
dATP	Sab-1	0.049 ± 0.0008	1.22	1.239 ± 0.020	6.19	0.040	5.10
	Tan-1	0.059 ± 0.0019		7.677 ± 0.100		0.008	
dGTP	Sab-1	0.030 ± 0.0002	1.56	1.132 ± 0.206	7.18	0.027	4.60
	Tan-1	0.048 ± 0.0006		8.125 ± 0.198		0.006	

FIGURE 2: Pre-steady state kinetic parameters of Sab-1 and Tan-1 RT proteins. (A) Active site concentrations of Sab-1 and Tan-1 RTs. The ^{32}P-labeled 23-mer primer (300 nM) annealed to the 38-mer RNA template (1:2 for P/T) was prebound to 50−75 nM active RTs and was rapidly mixed with 800 μM dTTP, followed by a quench reaction with EDTA (50 mM). Pre-steady state kinetic data were analyzed using nonlinear regression. The active concentration of Sab-1 RT was 92.1 ± 2.3 nM based on an initial Sab-1 RT protein concentration of 150 nM. The preparation of Sab-1 RT used to perform further pre-steady state analysis was 61.4% active protein. The active concentration of Tan-1 RT was 27.8 ± 1.5 nM based on an initial Tan-1 RT protein concentration of 92.5 nM. The preparation of Tan-1 RT used to complete the pre-steady state analysis was 30% active protein. (B) Pre-steady state dCTP titration curves for Sab-1 and Tan-1 RTs. The ^{32}P-labeled 23-mer C primer annealed to the 38-mer RNA template (50 nM) was extended with 200 nM active RT for single-round dCTP incorporation at six different dCTP concentrations. Data from single-turnover experiments were fit to a single-exponential equation that measures the rate of dNTP incorporation (k_{obsd}) per given dNTP concentration. These results were then used to determine K_d, the dissociation constant for binding of dNTP to the RT−T/P binary complex, and k_{pol}, the maximum rate of conformational change or chemical catalysis. (C) Summarized K_d and k_{pol} values of Tan-1 and Sab-1 RTs with four dNTPs.

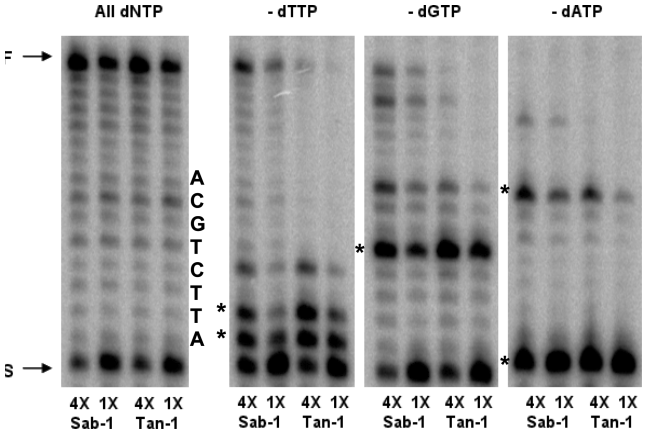

FIGURE 3: Misincorporation assay for Sab-1 and Tan-1 RT proteins with biased dNTP pools. Primer extension assays were used to determine the misincorporation ability of both SIVagm RTs. The 23-mer Extend T primer (5′-CGCGCCGAATTCCCGCTAG-CAAT-3′, S) annealed to the 38-mer RNA template was extended with five different dNTP compositions (all four dNTPs and one of the four dNTPs deleted) for 5 min at 37 °C. The same two RT activities, 4× and 1×, showing approximately 75 and 25% full-length extension (F), respectively, were used. The reaction mixtures were analyzed with 14% denaturing polyacrylamide gels. The stop sites are marked with asterisks, and the sequence of the synthesized DNA was also labeled.

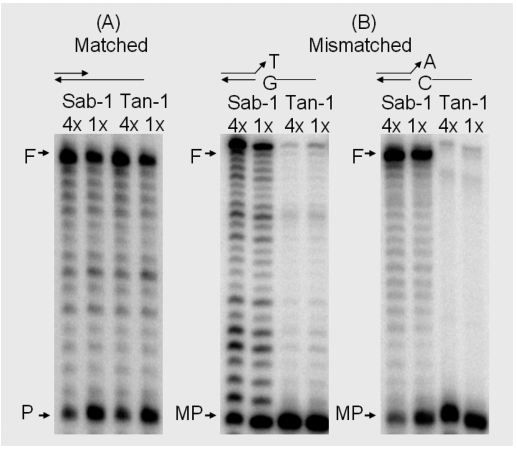

FIGURE 4: Mismatch extension capability of Sab-1 and Tan-1 RT proteins. (A) The ^{32}P-labeled matched primer (P) annealed to the 38-mer RNA template was extended by two different concentrations of Sab-1 and Tan-1 RTs showing approximately 25% (1×) and 75% (4×) primer extension (F) at 37 °C for 5 min with 250 μM dNTP. (B) The primer extension reactions were repeated with mismatched primers (MP) annealed to the 38-mer RNA (G/T) or DNA template (C/A), under the same condition used in the matched T/P reactions. The reaction mixtures were analyzed with 14% denaturing polyacrylamide gels.

efficient (k_{pol}/K_d) at incorporating a nucleotide than Sab-1 RT. This illustrates that Tan-1 RT exhibits a lower dNTP binding affinity (K_d) than Sab-1 RT, which mechanistically explains why Tan-1 RT displayed limited DNA synthesis efficiency at low dNTP concentrations (Figure 1).

Fidelity Comparison between Sab-1 and Tan-1 RT Proteins. We previously reported that, with two reduced dNTP binding mutants of HIV-1 RT, Q151N and V148I, a reduction in the dNTP binding affinity of RT elevates the enzyme fidelity (*20*, *23*). Thus, we next tested the ability of Sab-1 and Tan-1 RT proteins to polymerize DNA in biased dNTP pools, which is indicative of the enzyme's fidelity. The ^{32}P-labeled 17-mer primer annealed to the 38-mer RNA template used in Figure 1 was extended for 5 min at 37 °C in the absence of one of the four dNTPs (see Figure 3) by an equal polymerase activity of each RT (determined by the primer extension with all four dNTPs as described in the legend of Figure 1). Under this condition, the primer extension stops at one nucleotide before the sites where the deleted dNTP should have been incorporated, called the stop site (see the asterisks in Figure 3). Theoretically, under these conditions, higher-fidelity RTs display less extension beyond the stop site than low-fidelity RTs with greater capability to incorporate incorrect dNTPs and extend the produced mismatched primer (*19*, *30*−*32*). As shown in Figure 3, the ability of Sab-1 RT to extend the primer beyond the stop sites was greater than that of Tan-1 RT (minus dCTP reaction data not shown), indicating that Tan-1 RT is less error prone than Sab-1 RT. Lastly, we tested the mismatch extension fidelity of Sab-1 and Tan-1 RTs. Two sets of mismatched T/P substrates were used to assess the ability of each RT to extend a mismatched T/P on RNA (G/T) or DNA (C/A) templates (Figure 4). With an equal polymerase activity (determined with the matched T/P), Tan-1 RT exhibited a weak ability to extend either mismatched T/P substrate compared to Sab-1 RT. This indicates that Tan-1 RT has a higher mismatch extension fidelity than Sab-1 RT. The ability to extend mismatched T/P substrates has been shown to play a crucial role in modulating DNA polymerase fidelity (*19*, *20*).

Test for the Roles of the C148 Residue of Tan-1 RT in dNTP Incorporation Kinetics and Fidelity. Previously, we reported that RT of a SIVMNE 170 clone, which was isolated from an animal infected with a cloned SIVMNE CL8 strain 170 weeks post-infection, displays elevated fidelity and reduced dNTP incorporation efficiency, compared to those of SIVMNE CL8 RT (*18*). Importantly, we found that a specific mutation, V148I, of SIVMNE 170 RT is fully responsible for the decreased dNTP binding affinity and elevated fidelity of the 170 RT, suggesting that the V148 residue, which is encoded in the conserved "VLPQ" b8−αE loop region of RT, is essential for the low-fidelity and tight dNTP binding natures of SIVMNE CL8 RT (*18*, *30*). Interestingly, Tan-1 RT has a cysteine residue at position 148, whereas like SIVMNE CL8 RT, Sab-1 RT has a valine residue. Thus, we tested if the cysteine sequence of Tan-1 RT contributes to the high-fidelity and low-dNTP utilization efficiency nature of Tan-1 RT. For this test, we replaced the C148 residue of Tan-1 RT with valine (C148V), and we compared the dNTP utilization efficiency (Figure 5A) and fidelity (Figure 5B) of this mutant with those of a parental Tan-1 RT containing the C148 residue. As shown in Figure 5A, the C148V mutant of Tan-1 RT exhibited little difference in dNTP incorporation efficiency (see the dNTP concentration showing 50% activity reduction, asterisks). Furthermore, the C148V Tan-1 RT displayed no significant difference in the misincorporation assay with biased dNTP pools (Figure 5B). These data suggest that, unlike a pair of SIVMNE RT proteins that we previously studied, the valine sequence at position 148 is not involved in the elevated fidelity and reduced dNTP incorporation efficiency of Tan-1 RT, and likely, other sequence variations specific for Tan-1 RT are involved in the biochemical differences observed between Tan-1 RT and Sab-1 RT.

DISCUSSION

In this work, we demonstrated that RTs of the five natural SIVagm strains isolated from four different AGM species, which uniquely dwell at different regions of Africa, have varying dNTP

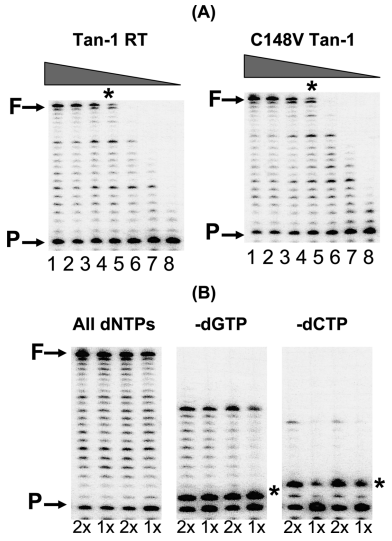

FIGURE 5: dNTP concentration-dependent polymerase activity and misincorporation capability of Tan-1 RT and C148V Tan-1 RT. (A) dNTP incorporation efficiency assay. The 5′-end ^{32}P-labeled primer (P) annealed to the 38-mer RNA template was extended by an equal activity of Tan-1 RT and C148V Tan-1 RT with a high dNTP concentration (50 μM). The reactions were repeated with eight decreasing dNTP concentrations (25, 5, 1, 0.5, 0.25, 0.1, 0.05, and 0.025 μM). The dNTP concentrations displaying approximately 50% primer extension shown with 50 μM dNTP (F) are marked with asterisks. (B) Misincorporation assay. The 5′-end ^{32}P-labeled 17-mer primer annealed to the 38-mer RNA template was extended by two equal activities (2× and 1×) of Tan-1 and C148V Tan-1 RT proteins determined in the presence of all dNTPs (250 μM), and then the reactions were repeated in the presence of two biased dNTP pools (without dGTP and without dCTP) at 37 °C for 5 min. The reaction mixtures were analyzed with 14% urea denaturing gels. The first stop sites generated by the omission of each dNTP are marked with asterisks.

utilization efficiencies. Among them, Sab-1 and Tan-1 RTs exhibit the largest difference in dNTP utilization efficiency, which results from their dNTP binding affinity differences, instead of the conformational change or catalysis step. In addition, Tan-1 RT displays higher enzyme fidelity than Sab-1 RT. Interestingly, these concomitant dNTP binding affinity and fidelity alterations were also observed when HIV-1 and MuLV RTs were compared. MuLV RT has 10−120-fold lower dNTP binding affinity and higher enzyme fidelity than HIV-1 RT, particularly the mismatch extension fidelity (*19*). Tan-1 RT appears to mechanistically mimic MuLV RT even though Tan-1 RT is a lentiviral RT. We also previously reported on the RTs of two SIV variants, SIVMNE CL8 and SIVMNE170, which were isolated from a single infected animal, but at different time points post-infection (*18*, *30*, *33*). They also showed different dNTP binding affinity and fidelity (*30*), and SIVMNE170 RT biochemically behaves like SIVagm Tan-1 RT (low dNTP binding affinity and less error prone). Therefore, with the data presented in this report, it is increasingly apparent that biochemical properties of lentiviral RTs such as dNTP binding affinity and enzyme fidelity can vary both between and within host species. However, unlike the case of SIVMNE RT proteins, our data support the possibility that the Val 148 residue is not involved in the observed mechanistic characteristics of Tan-1 RT, suggesting that structural elements involved in the mechanistic difference between Sab-1 and Tan-1 RTs are different from those between the two SIVMNE RTs. The amino acid sequence identity and similarity among three subdomains of the Sab-1 and Tan-1 RT polymerase domains, fingers (residues 1−90), palm (residues 91−225), and thumb (residues 226−325), are 63 and 87%, 65 and 85%, and 66 and 93%, respectively. Therefore, it is possible that there could be multiple sequence variations between the DNA polymerase domains of these two SIVagm RTs that affect the mechanistic difference observed in this study.

Unlike the extensive studies on the *Env* gene of lentiviruses, the virological consequences created by the biochemical alterations of RT described in this study remain to be explored. A hint about one possible consequence was presented when we observed that, unlike the wild-type HIV-1 vector, the HIV-1 vectors harboring HIV-1 RT mutants with reduced dNTP affinity such as V148I and Q151N efficiently transduced T cells and other dividing cells but failed to transduce terminally differentiated or nondividing macrophages (*34*). This was later explained to be due to the extremely low concentrations of cellular dNTPs in macrophages (~40 nM) at which the V148I and Q151N HIV-1 RTs have poor enzymatic activity (*35*). Therefore, we can envision that SIVagm Tan-1 may display lower macrophage infectivity than SIVagm Sab-1 because Tan-1 RT exhibits significantly lower dNTP activity at 40 nM dNTP (see Figure 1). Thus, Tan-1 would preferentially infect T cells harboring sufficient dNTP pools. However, this issue currently needs to be tested, and other determinants for cell tropism such as *Env* and *Vpr* also need to be considered. In conclusion, it is increasingly apparent that biochemical alterations may occur in RT of lentiviruses during natural viral propagation.

REFERENCES

1. Coffin, J. M. (1986) Genetic variation in AIDS viruses. *Cell 46*, 1–4.
2. Coffin, J. M. (1992) Genetic diversity and evolution of retroviruses. *Curr. Top. Microbiol. Immunol. 176*, 143–164.
3. Coffin, J. M. (1995) HIV population dynamics in vivo: Implications for genetic variation, pathogenesis, and therapy. *Science 267*, 483–489.
4. Goudsmit, J., Back, N. K., and Nara, P. L. (1991) Genomic diversity and antigenic variation of HIV-1: Links between pathogenesis, epidemiology and vaccine development. *FASEB J. 5*, 2427–2436.
5. Zhang, L., Carruthers, C. D., He, T., Huang, Y., Cao, Y., Wang, G., Hahn, B., and Ho, D. D. (1997) HIV type 1 subtypes, coreceptor usage, and CCR5 polymorphism. *AIDS Res. Hum. Retroviruses 13*, 1357–1366.
6. Kirchhoff, F., Mori, K., and Desrosiers, R. C. (1994) The "V3" domain is a determinant of simian immunodeficiency virus cell tropism. *J. Virol. 68*, 3682–3692.
7. Shioda, T., Oka, S., Ida, S., Nokihara, K., Toriyoshi, H., Mori, S., Takebe, Y., Kimura, S., Shimada, K., and Nagai, Y.; et al. (1994) A naturally occurring single basic amino acid substitution in the V3 region of the human immunodeficiency virus type 1 env protein alters the cellular host range and antigenic structure of the virus. *J. Virol. 68*, 7689–7696.
8. Baier, M., Werner, A., Cichutek, K., Garber, C., Muller, C., Kraus, G., Ferdinand, F. J., Hartung, S., Papas, T. S., and Kurth, R. (1989) Molecularly cloned simian immunodeficiency virus SIVagm3 is highly divergent from other SIVagm isolates and is biologically active in vitro and in vivo. *J. Virol. 63*, 5119–5123.
9. Fomsgaard, A., Hirsch, V. M., Allan, J. S., and Johnson, P. R. (1991) A highly divergent proviral DNA clone of SIV from a distinct species of African green monkey. *Virology 182*, 397–402.
10. Fukasawa, M., Miura, T., Hasegawa, A., Morikawa, S., Tsujimoto, H., Miki, K., Kitamura, T., and Hayami, M. (1988) Sequence of simian immunodeficiency virus from African green monkey, a new member of the HIV/SIV group. *Nature 333*, 457–461.
11. Johnson, P. R., Fomsgaard, A., Allan, J., Gravell, M., London, W. T., Olmsted, R. A., and Hirsch, V. M. (1990) Simian immunodeficiency viruses from African green monkeys display unusual genetic diversity. *J. Virol. 64*, 1086–1092.
12. Li, Y., Naidu, Y. M., Daniel, M. D., and Desrosiers, R. C. (1989) Extensive genetic variability of simian immunodeficiency virus from African green monkeys. *J. Virol. 63*, 1800–1802.

13. Li, Y., Naidu, Y., Fultz, P., Daniel, M. D., and Desrosiers, R. C. (1989) Genetic diversity of simian immunodeficiency virus. *J. Med. Primatol. 18*, 261–269.
14. Wertheim, J. O., and Worobey, M. (2007) A challenge to the ancient origin of SIVagm based on African green monkey mitochondrial genomes. *PLoS Pathog. 3*, e95.
15. Allan, J. S., Short, M., Taylor, M. E., Su, S., Hirsch, V. M., Johnson, P. R., Shaw, G. M., and Hahn, B. H. (1991) Species-specific diversity among simian immunodeficiency viruses from African green monkeys. *J. Virol. 65*, 2816–2828.
16. Kim, B. (1997) Genetic selection in *Escherichia coli* for active human immunodeficiency virus reverse transcriptase mutants. *Methods 12*, 318–324.
17. Kim, B., Hathaway, T. R., and Loeb, L. A. (1996) Human immunodeficiency virus reverse transcriptase. Functional mutants obtained by random mutagenesis coupled with genetic selection in *Escherichia coli*. *J. Biol. Chem. 271*, 4872–4878.
18. Diamond, T. L., Kimata, J., and Kim, B. (2001) Identification of a simian immunodeficiency virus reverse transcriptase variant with enhanced replicational fidelity in the late stage of viral infection. *J. Biol. Chem. 276*, 23624–23631.
19. Skasko, M., Weiss, K. K., Reynolds, H. M., Jamburuthugoda, V., Lee, K., and Kim, B. (2005) Mechanistic differences in RNA-dependent DNA polymerization and fidelity between murine leukemia virus and HIV-1 reverse transcriptases. *J. Biol. Chem. 280*, 12190–12200.
20. Weiss, K. K., Chen, R., Skasko, M., Reynolds, H. M., Lee, K., Bambara, R. A., Mansky, L. M., and Kim, B. (2004) A role for dNTP binding of human immunodeficiency virus type 1 reverse transcriptase in viral mutagenesis. *Biochemistry 43*, 4490–4500.
21. Johnson, K. A. (1995) Rapid quench kinetic analysis of polymerases, adenosinetriphosphatases, and enzyme intermediates. *Methods Enzymol. 249*, 38–61.
22. Kati, W. M., Johnson, K. A., Jerva, L. F., and Anderson, K. S. (1992) Mechanism and fidelity of HIV reverse transcriptase. *J. Biol. Chem. 267*, 25988–25997.
23. Weiss, K. K., Bambara, R. A., and Kim, B. (2002) Mechanistic role of residue Gln151 in error prone DNA synthesis by human immunodeficiency virus type 1 (HIV-1) reverse transcriptase (RT). Pre-steady state kinetic study of the Q151N HIV-1 RT mutant with increased fidelity. *J. Biol. Chem. 277*, 22662–22669.
24. Johnson, K. A. (1993) Conformational coupling in DNA polymerase fidelity. *Annu. Rev. Biochem. 62*, 685–713.
25. Kerr, S. G., and Anderson, K. S. (1997) Pre-steady-state kinetic characterization of wild type and 3′-azido-3′-deoxythymidine (AZT) resistant human immunodeficiency virus type 1 reverse transcriptase: Implication of RNA directed DNA polymerization in the mechanism of AZT resistance. *Biochemistry 36*, 14064–14070.
26. Feng, J. Y., and Anderson, K. S. (1999) Mechanistic studies examining the efficiency and fidelity of DNA synthesis by the 3TC-resistant mutant (184V) of HIV-1 reverse transcriptase. *Biochemistry 38*, 9440–9448.
27. Hirsch, V. M., Dapolito, G., Johnson, P. R., Elkins, W. R., London, W. T., Montali, R. J., Goldstein, S., and Brown, C. (1995) Induction of AIDS by simian immunodeficiency virus from an African green monkey: Species-specific variation in pathogenicity correlates with the extent of in vivo replication. *J. Virol. 69*, 955–967.
28. Jin, M. J., Hui, H., Robertson, D. L., Muller, M. C., Barre-Sinoussi, F., Hirsch, V. M., Allan, J. S., Shaw, G. M., Sharp, P. M., and Hahn, B. H. (1994) Mosaic genome structure of simian immunodeficiency virus from west African green monkeys. *EMBO J. 13*, 2935–2947.
29. Soares, M. A., Robertson, D. L., Hui, H., Allan, J. S., Shaw, G. M., and Hahn, B. H. (1997) A full-length and replication-competent proviral clone of SIVAGM from tantalus monkeys. *Virology 228*, 394–399.
30. Diamond, T. L., Souroullas, G., Weiss, K. K., Lee, K. Y., Bambara, R. A., Dewhurst, S., and Kim, B. (2003) Mechanistic Understanding of an Altered Fidelity Simian Immunodeficiency Virus Reverse Transcriptase Mutation, V148I, Identified in a Pig-tailed Macaque. *J. Biol. Chem. 278*, 29913–29924.
31. Weiss, K. K., Isaacs, S. J., Tran, N. H., Adman, E. T., and Kim, B. (2000) Molecular architecture of the mutagenic active site of human immunodeficiency virus type 1 reverse transcriptase: Roles of the β8-αE loop in fidelity, processivity, and substrate interactions. *Biochemistry 39*, 10684–10694.
32. Operario, D. J., Reynolds, H. M., and Kim, B. (2005) Comparison of DNA polymerase activities between recombinant feline immunodeficiency and leukemia virus reverse transcriptases. *Virology 335*, 106–121.
33. Kimata, J. T., Kuller, L., Anderson, D. B., Dailey, P., and Overbaugh, J. (1999) Emerging cytopathic and antigenic simian immunodeficiency virus variants influence AIDS progression. *Nat. Med. 5*, 535–541.
34. Diamond, T. L., Roshal, M., Jamburuthugoda, V. K., Reynolds, H. M., Merriam, A. R., Lee, K. Y., Balakrishnan, M., Bambara, R. A., Planelles, V., Dewhurst, S., and Kim, B. (2004) Macrophage tropism of HIV-1 depends upon efficient cellular dNTP utilization by reverse transcriptase. *J. Biol. Chem. 279*, 51545–51553.
35. Jamburuthugoda, V. K., Chugh, P., and Kim, B. (2006) Modification of human immunodeficiency virus type 1 reverse transcriptase to target cells with elevated cellular dNTP concentrations. *J. Biol. Chem. 281*, 13388–13395.